The role of grain-boundary cementite in bainite formation in high-carbon steels

Ravi, Ashwath M.; Sietsma, Jilt; Santofimia, Maria J.

DOI
10.1016/j.scriptamat.2020.03.042

Publication date
2020

Document Version
Final published version

Published in
Scripta Materialia

Scripta Materialia 185 (2020) 7–11

Contents lists available at ScienceDirect

Scripta Materialia

journal homepage: www.elsevier.com/locate/scriptamat

The role of grain-boundary cementite in bainite formation in high-carbon steels

Ashwath M. Ravi*, Jilt Sietsma, Maria J. Santofimia

Dept. of Materials Science and Engineering, Delft University of Technology, Mekelweg 2, Delft 2628 CD, the Netherlands

ARTICLE INFO

Article history:
Received 28 December 2019
Revised 18 March 2020
Accepted 19 March 2020

Keywords:
Bainite
Kinetics
Nucleation
Isothermal heat treatments
Grain-boundary cementite

ABSTRACT

Low temperature bainite formation in high-carbon steels leads to highly refined microstructures. However, the rate of bainite formation becomes impractically low as the bainite formation temperature decreases. Thus, it is important to create strategies to accelerate the low-temperature bainite formation kinetics in high-carbon steels. In this work, it is observed that decorating the parent austenite grain boundaries with grain-boundary cementite prior to bainite formation leads to an appreciable acceleration of subsequent bainite formation kinetics due to decrease in activation energy for bainite nucleation at cemenite/austenite interfaces.

Bainite microstructures typically consist of series of bainitic ferrite laths [1–4]. Studies show that the bainitic laths become finer as the transformation temperature decreases [3–5]. Lowering the bainite formation temperature, however, leads to extremely slow bainite formation kinetics, especially in high carbon steels with total transformation times ranging from a few hours to over several days [6,7]. This has prompted researchers to explore strategies for accelerating the low-temperature bainite formation kinetics [6]. Studies show that the rate of bainite formation increases with decreasing parent austenite grain size [1,8,9]. However, this trend is not universally applicable. Some studies show that the rate of bainite formation increases with increasing parent austenite grain size [10–12]. Other strategies proposed in the literature for the acceleration of bainite formation kinetics include the formation of either grain-boundary ferrite [13,14] or martensite [15,16] prior to bainite formation. The formation of grain-boundary ferrite is thermodynamically not feasible in case of high-carbon steels, rendering the former strategy inapplicable. In the presence of pre-existing martensite, it is observed that the overall time for bainite formation is reduced [15–18]. However, since bainite formation treatment is typically carried out at temperatures higher than the quenching temperature where the initial martensite fraction is formed, an additional heating step is necessary [17,18]. Furthermore, compared to a fully bainitic microstructure, mechanical properties of martensite/bainite microstructures can be different [19,20] if the morphology and distribution of bainite is different from that of the surrounding martensite [19]. In this work, an alternative strategy based on the decoration of austenite grain boundaries with cementite precipitates is proposed for the acceleration of bainite formation kinetics in high-carbon steels. Such a strategy results in an almost fully bainitic microstructure without any additional heat treatment steps. Although networks of grain-boundary cementite can act as crack initiation and propagation sites [1], published results suggest that small isolated regions of grain-boundary cementite are not detrimental to the mechanical properties [21]. In this work, it is observed that a small fraction of isolated cementite precipitates can increase the rate of subsequent bainite formation significantly. The fundamental reasons behind such a trend are discussed in this work.

The composition of the high-carbon steel used in the present work is given in Table 1. The samples were heat treated using a Bähr DIL805A/D dilatometer according to the time-temperature parameters given in Fig. 1. It can be observed that the austenitization treatment was carried out at 1000 °C for 5 minutes. Preliminary experimental investigations reveal that such an austenitization treatment is sufficient to dissolve all the carbides present in starting microstructure. Furthermore, the A_{cm} temperature was calculated to be 927 °C based on Thermo-Calc calculations. Bainite formation treatments were carried out directly after austenization in some samples while in others, an intermediate annealing treatment (IAT) prior to the bainite formation was employed. The IAT temperatures were chosen such that the austenite grain bound-

* Corresponding author.
E-mail addresses: ashwath.ravi@tatasteeleurope.com (A.M. Ravi), J.Sietsma@tudelft.nl (J. Sietsma), M.J.SantofimiaNavarro@tudelft.nl (M.J. Santofimia).

https://doi.org/10.1016/j.scriptamat.2020.03.042
1359-6462/

Table 1
Chemical composition of the steel used for study (values in wt%).

C	Mn	Si	Cr	Cu	Mo	Ni	V
1.05	0.274	0.278	1.67	0.030	0.012	0.042	0.016

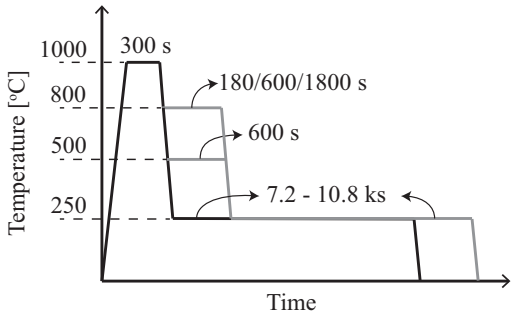

Fig. 1. Schematic of heat treatment profiles used for understanding the effect of grain-boundary cementite precipitation on bainite formation kinetics. The heating rate used during the heat treatments is 5 °C/s while the all cooling steps are carried out at −40 °C/s.

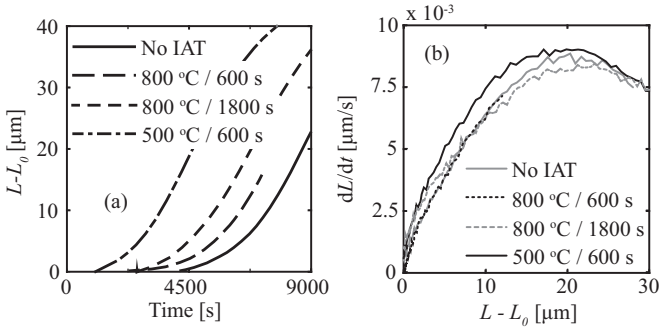

Fig. 2. (a) Bainite evolution obtained via different heat treatment routes represented in terms of change in length of the sample during isothermal holding at 250 °C (b) Rate of change of length of sample as a function of sample expansion during isothermal holding at 250 °C. No IAT refers to the heat treatment where IAT was not applied prior to bainite formation. The rest of the curves were obtained after an IAT was employed. The time and temperature of the IAT is mentioned in the legend.

ary will be decorated with a small fraction of cementite based on Thermo-Calc calculations. Bainite formation temperature for all samples was 250 °C. The samples were held at this temperature of 2–3 h. It should also be noted that the experimentally determined M_s temperature is approximately 150 °C. The heat treated samples were studied using optical microscopy and scanning electron microscopy (SEM).

The kinetics of bainite formation during the different heat treatments are compiled in Fig. 2. In Fig. 2(a), bainite formation as a function of time is represented in terms of change in length of the sample as a function of time during the isothermal holding at 250 °C. Similar procedure has been previously used in [10,22].

Fig. 2(a) shows that the bainite formation is accelerated when a prior IAT is applied. Moreover, the degree of acceleration of bainite formation can be observed to increase as the IAT temperature decreases. Similarly, the time required for bainite formation at 250 °C also decreases as holding time during IAT increases.

Fig. 2(b) shows the rate of change of the dilatometer sample length as a function of change in sample length during bainite formation at 250 °C after various intermediate annealing conditions. Since the change in length of the sample represents the volume fraction of bainite formed, Fig. 2(b) essentially gives the rate of bainite formation as a function of bainite fraction. It is interesting to see that, although the overall time for bainite formation decreases when an IAT is employed prior to bainite formation, the instantaneous rate of bainite formation as a function of bainite fraction is similar in all cases. This implies that the overall time required of bainite formation after IAT is lower since the onset of bainite formation takes place earlier in time compared to when bainite forms without an IAT. However, after the transformation has begun, the bainite formation rate is similar in all cases.

Fig. 3 shows the results obtained from the microstructural studies. Fig. 3(a) shows that a lower-bainite and martensite/retained austenite microstructure is obtained after a low-temperature bainite formation treatment at 250 °C without any prior IAT. Nital etching used to reveal the microstructure selectively etches bainitic regions while fresh martensite and retained austenite remain unetched. Dilatometry results show that the austenite to bainite transformation is not yet completed during the time frame of the experiment (2–3 h isothermal holding at 250 °C) and the residual austenite partially transforms into martensite upon the final cooling to room temperature. This is evident in the obtained microstructure. Fig. 3(b) and (c) show the resultant microstructure when bainite formation is carried out following IATs for 10 min at 800 °C and 500 °C respectively. These figures also show a lower-bainite and martensite/retained austenite microstructure. Additionally, grain-boundary cementite precipitates are observed at the parent austenite grain boundaries when an IAT is used as indicated in Fig. 3(b) and (c). The fraction of the grain-boundary cementite precipitates is higher when IAT is carried out at 500 °C than at 800 °C.

Based on these results, it can be concluded that the grain-boundary cementite formed during the IAT decreases the time required for the onset of bainite formation and leads to faster overall bainite formation kinetics in high carbon steels. Umemoto et al. also reported that cementite precipitation leads to faster bainite formation kinetics in medium carbon steels [23]. However, they did

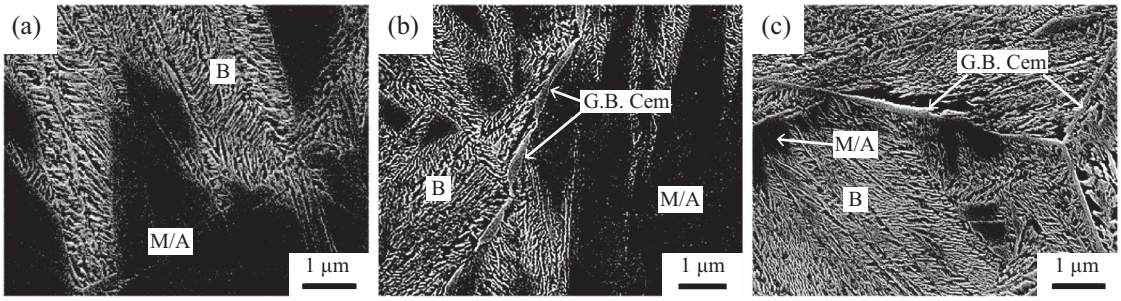

Fig. 3. SEM micrographs obtained after bainite formation treatment when it preceded by (a) no IAT (b) IAT at 500 °C for 10 min and (c) IAT at 800 °C for 10 min. Microstructure studies revealed Bainite (B), Martensite/Retained austenite (M/A) islands and grain-boundary cementite (G.B. Cem) depending on the corresponding treatment route.

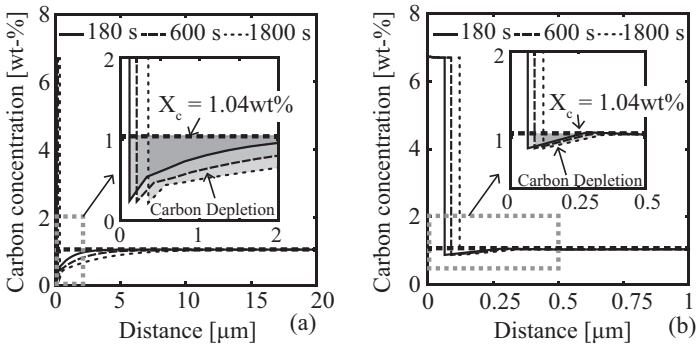

Fig. 4. Variation in carbon concentration in the vicinity of cementite/austenite interface as a result of cementite precipitation after isothermal holding at (a) 500 °C and (b) 800 °C for different times based on DICTRA calculations simulating IAT. Shaded regions indicate the carbon depleted regions. Simulations indicate moving cementite/austenite interface during the time-scale of IAT as well as a higher fraction of cementite formation during IAT at 500 °C.

not indicate if such faster kinetics is the result of earlier onset of bainite formation as seen in this work. Additionally, the fundamental reason behind such a trend is not studied in their work. Nevertheless, understanding the mechanism is essential to effectively use grain-boundary cementite to accelerate bainite formation kinetics. In subsequent paragraphs, the underlying reason behind the decrease in the time required for the onset of bainite formation in the presence of grain-boundary cementite is investigated.

The rate of bainite formation depends on the nucleation kinetics of bainite [24,25] which is determined by the activation energy for the nucleation process [24–31]. The activation energy for bainite nucleation depends on the thermodynamic conditions at nucleation sites. The precipitation of grain-boundary cementite affects the carbon concentration in the vicinity of the cementite/austenite interface. Fig. 4 shows the distribution of carbon during cementite formation in austenite for various times at 800 °C and 500 °C. The carbon profile was calculated using multi-component diffusion simulations performed with DICTRA. 1-D isothermal holding simulations at 800 °C and 500 °C assuming local equilibrium at the cementite/austenite interface were carried out to replicate the IAT. A simulation cell assuming an initial austenite size of 60μm (austenite grain size after the austenitization treatment) and a cementite size of 1nm was used for the simulations. Simulations were carried out in a system with a composition identical to the steel composition given in Table 1 with the exception of Cu since the exceptionally low solubility of Cu [32] in cementite led to convergence problems. Excluding Cu is not expected to affect the results since the concentration of Cu (0.03 wt%) in the steel used in this study is extremely low. Additionally, experimental studies suggest that Cu does not affect the formation of cementite [32] even if present in higher concentrations. Wasynczuk et al. suggest that Cu partitions out during cementite formation as ϵ-Cu precipitates at cementite/austenite interfaces [32]. Published results indicate that the cementite/austenite interface is faceted and ϵ-Cu precipitates only along the partially coherent and immobile facets of the cementite/austenite interface [32,33]. Thus, ϵ-Cu precipitation does not impede the migration of mobile regions of cementite/austenite interfaces [32].

Fig. 4 shows that a higher cementite fraction is formed at 500 °C than at 800 °C. The steep decrease in carbon concentration in Fig. 4 indicates the position of the cementite/austenite interface, which gives insight into the growth of cementite precipitates during IATs. In DICTRA simulations, the thickness of cemenite (Fig. 4) in comparision to the overall size of the simulation cell can be interpreted as the fraction of cementite formed. These results are in line with the experimental results which suggest a higher fraction of grain-boundary cementite when the IAT temperature is lower. Fig. 4 suggests that cementite precipitates continually grow within the time scale of the IATs used in this work. Fig. 4 also shows that the precipitation of cementite leads to depletion of carbon in the austenite matrix in the vicinity of the cementite/austenite interface. This trend can be explained by the growth of carbon-rich cementite which leads to local decrease in carbon concentration in the vicinity of cementite/austenite interfaces. The activation energy for bainite nucleation depends on the carbon concentration of the austenite matrix and it decreases with decreasing carbon content [29–31]. This implies that the activation energy for bainite nucleation at cemenite/austenite interfaces would be lower than the activation energy for bainite nucleation at austenite grain boundaries without grain-boundary cementite. Faster bainite formation with increasing fraction of cementite along the austenite grain boundaries as a result of IAT at 500 °C compared to 800 °C is also consistent with the above discussion.

Fig. 2(b) shows that the rate of bainite formation as a function of bainite fraction remains constant regardless of the presence of grain-boundary cementite and the overall acceleration of bainite formation is only due to faster onset of bainite formation as result of cementite precipitation during the IAT. The displacive and diffusionless theory of bainite formation suggests that bainitic subunits nucleate and grow initially at already existing interfaces (typically austenite grain boundaries [24,34] and in this case, cementite/austenite interfaces as well [8]). This leads to the creation of bainite/austenite interfaces. Bainite formation then continues autocatalytically at these newly created bainite/austenite interfaces [24,34]. Fig. 4 shows that the degree of carbon depletion within the austenite matrix decreases as the distance from the cementite/austenite interfaces increases. Thus, the activation energy for autocatalytic bainite nucleation, which is dependent on the carbon concentration of austenite in the vicinity of bainite/austenite interfaces, would be similar regardless of the presence of grain-boundary cementite during bainite formation. Furthermore, the cementite/austenite interfaces and the austenite grain boundaries only assist in the initiation of bainite formation. Upon the onset, bainite formation only occurs autocatalytically. This correlates well with Fig. 2(b) where the instantaneous rate of bainite formation is similar in the presence and absence of grain-boundary cementite. However, the onset of bainite formation is controlled by the activation energy for bainite nucleation at austenite grain boundaries and cementite/austenite interfaces. In the presence of cementite/austenite interfaces, the activation energy of bainite nucleation at these interfaces is lower and thus, the onset of bainite formation is quicker.

The overall decrease in activation energy of bainite nucleation required to achieve a quicker onset of bainite formation after a given IAT can be estimated by comparing the experimentally

Table 2
Effect of intermediate annealing treatment (IAT) on the start of bainite formation.

Case	t_s [in s]	ΔQ^{IAT} [in kJ/mol]	ΔX_C [in wt-%]
No IAT	4525		
IAT at 800 °C for 600 s	3323	1.34	0.015
IAT at 800 °C for 1800 s	2986	1.80	0.02
IAT at 500 °C for 600 s	1280	5.49	0.06

obtained kinetics during various heat treatments. Using the principles of modelling of bainite start curves proposed by Van Bohemen based on displacive and diffusionless mechanism of bainite formation [31], the time required for bainite formation to begin, t_s, at a given temperature can be given as

$$t_s \propto \frac{1}{\kappa} \quad \text{where} \quad \kappa \propto \exp\left(\frac{-Q}{RT}\right) \tag{1}$$

where κ is the rate parameter, R is the universal gas constant, T is the bainite formation temperature and Q is the overall activation energy for bainite nucleation at pre-existing interfaces such as austenite grain boundaries and cementite/austenite interfaces [31]. Using Eq. (1), the overall decrease in activation energy for bainite nucleation following a given IAT can be estimated by comparing the t_s value as a result of the particular IAT to the corresponding value without any IAT using

$$\frac{t_s^O}{t_s^{IAT}} = \exp\left(\frac{Q^O - Q^{IAT}}{RT}\right) = \exp\left(\frac{\Delta Q^{IAT}}{RT}\right) \tag{2}$$

t_s^{IAT} and t_s^O are the t_s values following a particular IAT and in the absence of any IAT, respectively. Q^O and Q^{IAT} are the activation energies in the absence of grain-boundary cementite (i.e., no IAT) and when bainite forms in the presence of grain-boundary cementite after a certain IAT, respectively. As indicated in Eq. (2), ΔQ^{IAT} is the difference between these activation energies.

In Table 2, the time required to achieve 0.5μm change in sample length at 250 °C as a result of various IATs is tabulated. It should be noted that overall change in length of the sample as a result bainite formation at 250 °C is over 40μm. Thus, it can be assumed that a 0.5μm change in length of the sample would represent the start of bainite formation (presumably around 1%). Thus, the times noted in Table 2 give the approximate t_s values under various conditions. Based on these experimentally obtained values, ΔQ^{IAT} can be calculated using Eq. (2) (Table 2). As expected, ΔQ^{IAT} increases with the increasing formation of grain-boundary cementite because of decreasing Q^{IAT}. Based on the ΔQ^{IAT} values, the expected decrease in the carbon concentration in the vicinity of cementite/austenite interfaces can be calculated as well. The influence of chemical composition of austenite on activation energy for bainite nucleation has been empirically calculated in the literature as

$$Q_b = 89x_C + 10x_{Mn} + 12x_{Si} + 2x_{Cr} + 1x_{Ni} + 29x_{Mo} \tag{3}$$

where Q_b (in kJ/mol) is the contribution of the alloying elements to the total activation energy for bainite nucleation and x_i is concentration of element i in weight percent [31]. Using Eq. (3) and assuming that formation of grain-boundary cementite only affects the distribution of carbon, the decrease in carbon concentration in the austenite front of the cementite/austenite interface, ΔX_C can be calculated as

$$\Delta X_C = \frac{\Delta Q_{IAT}}{89} \tag{4}$$

ΔX_C values are also given in Table 2. It should be noted that DICTRA simulations suggest that the cementite forms under negligible-partitioning local equilibrium (NP-LE) regime at the IAT conditions used in this study. Table 2 shows that ΔX_C values are lower than the DICTRA-simulated carbon concentration in the vicinity of cementite/austenite interfaces (Fig. 4). This could be attributed to the extent of cementite precipitation. Microstructural studies reveal that the grain-boundary cementite is only precipitated on a portion of prior austenite grain boundaries and rest of prior austenite grain boundaries do not show any grain-boundary cementite. It should be noted that ΔX_C is calculated based on ΔQ^{IAT}, which depends on the activation energy for bainite nucleation at austenite grain boundaries and at cementite/austenite interfaces. DICTRA calculations only give the local decrease in carbon concentration at the cementite/austenite interface. It can be envisaged that if austenite grain boundaries were completely replaced by cementite/austenite interfaces due to extensive cementite precipitation, ΔQ^{IAT} and consequently ΔX_C would be higher.

Summarizing the above results, it can be concluded that grain-boundary cementite precipitation accelerates the kinetics of bainite formation due to faster onset of bainite formation. Such an acceleration is mainly attributed to the decrease of the activation energy for bainite nucleation at cementite/austenite interfaces which can be achieved even with a small fraction of grain-boundary cementite. In terms of heat treatment design, controlled grain-boundary cementite precipitation can be achieved even during cooling from the austenitization temperature and thus eliminating the necessity of additional heat treatment steps to accelerate the low-temperature bainite formation kinetics in high-carbon steels.

Declaration of Competing Interest

The authors declare that they have no known competing financial interests or personal relationships that could have appeared to influence the work reported in this paper.

Acknowledgements

The research leading to these results has received funding from the European Research Council under the European Union's Seventh Framework Programme (FP/2007-2013) / ERC Grant Agreement n. [306292]. The authors would also like to thank Stefan van Bohemen (Tata Steel RD&T) for his assistance with chemical analysis to determine the composition of the steel used in this study.

References

[1] H.K.D.H. Bhadeshia, Matsci Series, IOM Communications, 2001.
[2] R.F. Hehemann, K.R. Kinsman, H.I. Aaronson, Metall. Trans. 3 (5) (1972) 1077–1094, doi:10.1007/BF02642439.
[3] I. Timokhina, H. Beladi, X. Xiong, Y. Adachi, P. Hodgson, Acta Mater. 59 (14) (2011) 5511–5522, doi:10.1016/j.actamat.2011.05.024.
[4] C. Garcia-Mateo, F.G. Caballero, ISIJ Int. 45 (11) (2005) 1736–1740, doi:10.2355/isijinternational.45.1736.
[5] S. Singh, H. Bhadeshia, Mater. Sci. Eng. 245 (1) (1998) 72–79, doi:10.1016/S0921-5093(97)00701-6.
[6] C. Garcia-Mateo, F.G. Caballero, H.K.D.H. Bhadeshia, ISIJ Int. 43 (11) (2003) 1821–1825, doi:10.2355/isijinternational.43.1821.
[7] T. Sourmail, V. Smanio, Acta Mater. 61 (7) (2013) 2639–2648, doi:10.1016/j.actamat.2013.01.044.
[8] M. Umemoto, K. Horiuchi, I. Tamura, Trans. ISIJ 22 (1982) 854–861, doi:10.2355/isijinternational1966.22.854.
[9] S.-J. Lee, J.-S. Park, Y.-K. Lee, Scr. Mater. 59 (1) (2008) 87–90, doi:10.1016/j.scriptamat.2008.02.036.
[10] A. Matsuzaki, H. Bhadeshia, Mater. Sci. Technol. 15 (5) (1999) 518–522, doi:10.1179/026708399101506210.
[11] F. Hu, P. Hodgson, K. Wu, Mater. Lett. 122 (2014) 240–243, doi:10.1016/j.matlet.2014.02.051.
[12] G. Xu, F. Liu, L. Wang, H. Hu, Scr. Mater. 68 (11) (2013) 833–836, doi:10.1016/j.scriptamat.2013.01.033.
[13] K. Zhu, H. Chen, J.-P. Masse, O. Bouaziz, G. Gachet, Acta Mater. 61 (16) (2013) 6025–6036, doi:10.1016/j.actamat.2013.06.043.
[14] D. Quidort, Y. Bréchet, Acta Mater. 49 (20) (2001) 4161–4170, doi:10.1016/S1359-6454(01)00316-0.
[15] H. Vetters, J. Dong, H. Bornas, F. Hoffmann, H.-W. Zoch, International Journal of Materials Research 97 (10) (2006) 1432–1440, doi:10.3139/146.101388.

[16] A. Navarro-López, J. Sietsma, M.J. Santofimia, Metall. Mater. Trans. A 47 (3) (2016) 1028–1039, doi:10.1007/s11661-015-3285-6.
[17] W. Gong, Y. Tomota, S. Harjo, Y. Su, K. Aizawa, Acta Mater. 85 (2015) 243–249, doi:10.1016/j.actamat.2014.11.029.
[18] H. Kawata, M. Takahashi, K. Hayashi, N. Sugiura, N. Yoshinaga, in: Materials Science Forum, 638, Trans Tech Publications, 2010, pp. 3307–3312. doi: 10.4028/www.scientific.net/MSF.638-642.3307.
[19] Y. Tomita, K. Okabayashi, Metall. Trans. A 16 (1) (1985) 73–82, doi:10.1007/BF02656714.
[20] P. Abbaszadeh, S. Kheirandish, H. Saghafian, M.H. Goodarzy, Mater. Res. 21 (1) (2017), doi:10.1590/1980-5373-mr-2017-0469.
[21] K. Han, D.V. Edmonds, G.D.W. Smith, Metall. Mater. Trans. A 32 (6) (2001) 1313–1324, doi:10.1007/s11661-001-0222-7.
[22] Y. Xu, G. Xu, X. Mao, G. Zhao, S. Bao, Metals 7 (330) (2017), doi:10.3390/met7090330.
[23] M. Umemoto, T. Furuhara, I. Tamura, Acta Metall. 34 (11) (1986) 2235–2245, doi:10.1016/0001-6160(86)90169-0.
[24] M.J. Santofimia, F.G. Caballero, C. Capdevila, C. Garcia-Mateo, C.G. de Andres, Mater. Trans. 47 (6) (2006) 1492–1500, doi:10.2320/matertrans.47.1492.
[25] H.K.D.H. Bhadeshia, J. Phys. 43 (1982) 443–448.
[26] D. Quidort, Y.J.M. Bréchet, ISIJ Int. 42 (9) (2002) 1010–1017, doi:10.2355/isijinternational.42.1010.
[27] G.I. Rees, H.K.D.H. Bhadeshia, Mater. Sci. Technol. 8 (11) (1992) 985–993, doi:10.1179/mst.1992.8.11.985.
[28] N.A. Chester, H.K.D.H. Bhadeshia, J. Phys. IV France 07 (C5) (1997) 41–46, doi:10.1051/jp4:1997506.
[29] A.M. Ravi, J. Sietsma, M.J. Santofimia, Acta Mater. 105 (2016) 155–164, doi:10.1016/j.actamat.2015.11.044.
[30] D. Quidort, Y. Bréchet, Scr. Mater. 47 (3) (2002) 151–156, doi:10.1016/S1359-6462(02)00121-5.
[31] S.M.C. van Bohemen, Metall. Mater. Trans. A 41 (2) (2010) 285–296, doi:10.1007/s11661-009-0106-9.
[32] J.A. Wasynczuk, R.M. Fisher, G. Thomas, Metall. Trans. A 17 (12) (1986) 2163–2173, doi:10.1007/BF02645914.
[33] F.A. Khalid, D.V. Edmonds, Metall. Trans. A 24 (4) (1993) 781–793, doi:10.1007/BF02656500.
[34] S.M.C. van Bohemen, J. Sietsma, Int. J. Mater. Res. 99 (7) (2008) 739–747, doi:10.3139/146.101695.